Randolph Glacier Inventory:
A Dataset of Global Glacier Outlines
Version: 3.0
7 April 2013

GLIMS Technical Report

Dataset Description

The Randolph Glacier Inventory (RGI) is a globally complete inventory of glacier outlines. It is supplemental to the Global Land Ice Measurements from Space initiative (GLIMS). Production of the RGI was motivated by the forthcoming Fifth Assessment Report of the Intergovernmental Panel on Climate Change (IPCC AR5) and the inventory is being released initially with little documentation in view of the IPCC's tight deadlines during 2012. Updates beyond the IPCC 2012 deadlines will take the form of additions to the database of GLIMS.

Version History

Version 1.0 of the Randolph Glacier Inventory was released in February 2012. An unofficial update to Version 1.0 was provided in April 2012 to replace several regions that had topology errors and repeated polygons. Version 2.0, released in June 2012, was quality-controlled to eliminate a number of flaws, and provides a uniform set of data fields for each glacier complex. Several outlines were also been improved, and a number were added in previously omitted regions. Version 2.0 also added shapefiles for its first-order and second-order regions, and a summary of global glacierized area on a 1°×1° grid.

Version 3.0 is an interm release representing the RGI as of 7 April 2013. The main improvements include identification of all tidewater basins, and delineation of glaciers from glacier complexes in nearly all regions. Full documentation of these changes is being prepared and will be released soon.

Data Distribution Policy

The Randolph Glacier Inventory (RGI 3.0) is made available under certain transitional usage constraints:

1) It is intended for the estimation of total ice volumes and glacier mass changes at global and large-regional scales;
2) It is not to be used for reporting that focuses primarily on the properties of the inventory itself, such as global size distributions, or area/elevation distributions of glaciers; and
3) It is not to be distributed.

Data Sources

The RGI is a combination of both new and existing published glacier outlines. New outlines were provided by the glaciological community in response to requests for data on the GLIMS and Cryolist e-mail listservers. We visualized the data in a GIS by overlaying outlines on modern satellite imagery, and assessed their quality relative to other available products. In several regions the outlines already in GLIMS were used for RGI. Data from the World Glacier Inventory (WGI, http://nsidc.org/data/docs/noaa/g01130_glacier_inventory/; WGI, 1989) and the related WGI-XF (Cogley, 2009) were used for some glaciers of northern Asia and other newly-covered regions, with outlines approximated by circles of area equaling those reported in the source. Where no other data were available we relied on data from the Digital Chart of the World (Danko, 1992).

Dataset Reference
The following reference should be used when citing RGI version 3.0:

Arendt, A., T. Bolch, J.G. Cogley, A. Gardner, J.-O. Hagen, R. Hock, G. Kaser, W.T. Pfeffer, G. Moholdt, F. Paul, V. Radić, L. Andreassen, S. Bajracharya, N. Barrand, M. Beedle, E. Berthier, R. Bhambri, A. Bliss, I. Brown, E. Burgess, D. Burgess, F. Cawkwell, T. Chinn, L. Copland, B. Davies, H. De Angelis, E. Dolgova, K. Filbert, R. Forester, A. Fountain, H. Frey, B. Giffen, N. Glasser, S. Gurney, W. Hagg, D. Hall, U.K. Haritashya, G. Hartmann, C. Helm, S. Herreid, I. Howat, G. Kapustin, T. Khromova, C. Kienholz, M. Koenig, J. Kohler, D. Kriegel, S. Kutuzov, I. Lavrentiev, R. LeBris, J. Lund, W. Manley, C. Mayer, E. Miles, X. Li, B. Menounos, A. Mercer, N. Moelg, P. Mool, G. Nosenko, A. Negrete, C. Nuth, R. Pettersson, A. Racoviteanu, R. Ranzi, P. Rastner, F. Rau, B. Raup, J. Rich, H. Rott, C. Schneider, Y. Seliverstov, M. Sharp, O. Sigurðsson, C. Stokes, R. Wheate, S. Winsvold, G. Wolken, F. Wyatt, N. Zheltyhina. 2012, Randolph Glacier Inventory [v3.0]: A Dataset of Global Glacier Outlines. Global Land Ice Measurements from Space, Boulder Colorado, USA. Digital Media.

The first 11 authors comprise an ad-hoc committee that was responsible for assembly of the RGI. The remaining authors are data contributors, listed in alphabetical order. Note that some of the 11 committee members also contributed data. Although efforts have been made to trace the names of GLIMS contributors whose outlines are now in RGI, it is possible that some have been missed. We also do not include the name of every contributor to the WGI or WGI-XF who provided information that may be incorporated in RGI. Interested users are encouraged to access the site http://glims.org/About/contributors.php for more information on GLIMS contributors, and http://nsidc.org/data/docs/noaa/g01130_glacier_inventory for more documentation on the WGI.

Region Definitions
We define 19 glacier regions drawn mostly from Radić and Hock (2010), with some small modifications (Figure 1).

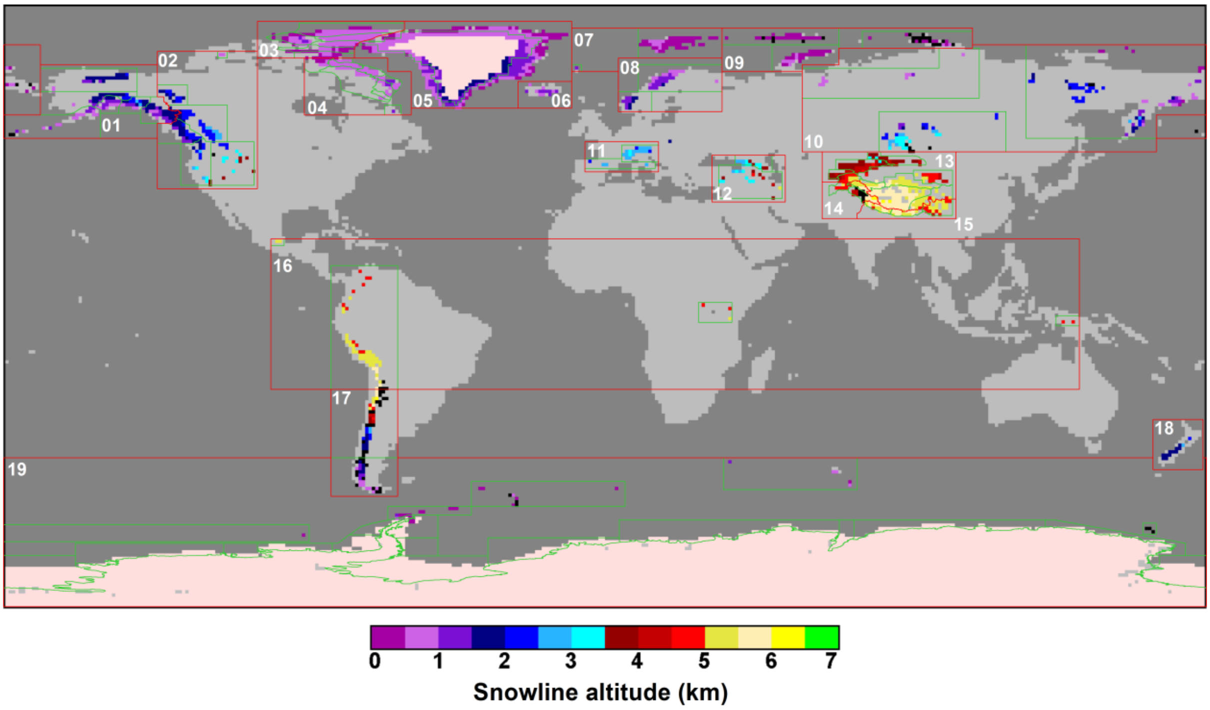

Figure 1. First-order regions (red) and second-order regions (green) of the Randolph Glacier Inventory, version 2.0.

First-order regions 01 and 10 straddle the 180th meridian, and so do second-order regions 01.03 and 19.15. For convenience of analysis in a cylindrical-equidistant coordinate system centred on longitude 0°, as in Figure 1, each of these regions appears in the accompanying shapefiles as two polygons, eastern and western.

Table 1. First-order and second-order regions of the Randolph Glacier Inventory, version 2.0.

Number	*Region*	*Code*	*Number*	*Subregion*
01.00	Alaska	ALA	01.01	N Alaska
			01.02	Alaska Ra (Wrangell/Kilbuck)
			01.03	Alaska Pena (Aleutians)
			01.04	W Chugach Mtns (Talkeetna)
			01.05	St Elias Mtns
			01.06	N Coast Ranges
02.00	Western Canada and USA	WNA	02.01	Melville Island
			02.02	Mackenzie and Selwyn Mtns
			02.03	S Coast Ranges
			02.04	N Rocky Mtns
			02.05	Cascade Ra and Sa Nevada
			02.06	S Rocky Mtns
03.00	Arctic Canada (North)	CDN	03.01	N Ellesmere Island
			03.02	Axel Heiberg and Meighen Is
			03.03	NC Ellesmere Island
			03.04	SC Ellesmere Island
			03.05	S Ellesmere Island (NW Devon)
			03.06	Devon Island
04.00	Arctic Canada (South)	CDS	04.01	Bylot Island
			04.02	W Baffin Island
			04.03	N Baffin Island
			04.04	NE Baffin Island
			04.05	EC Baffin Island
			04.06	SE Baffin Island
			04.07	Cumberland Sound
			04.08	Frobisher Bay
			04.09	Labrador
05.00	Greenland	GRE	05.01	Greenland (periphery)
			05.11	Greenland Ice Sheet
06.00	Iceland	ICE	06.00	Iceland
07.00	Svalbard and Jan Mayen	SVB	07.01	Svalbard
			07.02	Jan Mayen
08.00	Scandinavia	SCA	08.01	S Norway
			08.02	N Scandinavia
09.00	Russian Arctic	RAI	09.01	Franz Josef Land
			09.02	Novaya Zemlya
			09.03	Severnaya Zemlya
10.00	North Asia	NAS	10.01	North Asia (North)
			10.02	North Asia (East)
			10.03	E Chukotka
			10.04	Altay and Sayan
11.00	Central Europe	CEU	11.01	Alps

			11.02	Pyrenees and Apennines
12.00	Caucasus and Middle East	CAU	12.01	Greater Caucasus
			12.02	Middle East
13.00	Central Asia	CAN	13.01	Hissar Alay
			13.02	Pamir (Safed Khirs/W Tarim)
			13.03	W Tien Shan
			13.04	E Tien Shan (Dzhungaria)
			13.05	W Kun Lun
			13.06	E Kun Lun (Altyn Tagh)
			13.07	Qilian Shan
			13.08	Inner Tibet
			13.09	S and E Tibet
14.00	South Asia (West)	CAW	14.01	Hindu Kush
			14.02	Karakoram
			14.03	W Himalaya
15.00	South Asia (East)	CAS	15.01	C Himalaya
			15.02	E Himalaya
			15.03	Hengduan Shan
16.00	Low Latitudes	TRP	16.01	Low-latitude Andes
			16.02	Mexico
			16.03	E Africa
			16.04	New Guinea
17.00	Southern Andes	AND	17.01	Patagonia
			17.02	C Andes
18.00	New Zealand	NEZ	18.00	New Zealand
19.00	Antarctic and Subantarctic	ANT	19.01	Subantarctic (Pacific)
			19.02	South Shetlands and South Orkneys
			19.03	Subantarctic (Atlantic)
			19.04	Subantarctic (Indian)
			19.05	Balleny Islands
			19.11	E Queen Maud Land 7A
			19.12	Amery Ice Shelf 7B
			19.13	Wilkes Land 7C
			19.14	Victoria Land 7D
			19.15	Ross Ice Shelf 7E
			19.16	Marie Byrd Land 7F
			19.17	Pine Island Bay 7G
			19.18	Bellingshausen Sea 7H1
			19.19	Alexander Island 7H2
			19.20	W Antarctic Pena 7I1
			19.21	NE Antarctic Pena 7I2
			19.22	SE Antarctic Pena 7I3
			19.23	Ronne-Filchner Ice Shelf 7J
			19.24	W Queen Maud Land 7K
			19.31	Antarctic Ice Sheet

Technical Specifications

Data are provided as shapefiles containing the outlines of glaciers and glacier complexes in geographic coordinates (longitude/latitude, in degrees) and are referenced to the WGS84 datum. We define a glacier complex as a collection of contiguous glaciers that meet at glacier divides. Data are organized by first-order region, with one shapefile containing all glaciers for each region. For some of the regions included in this dataset, more detailed information about the glaciers is available from the GLIMS database or in the World Glacier Inventory (WGI).

Data Fields

Each glacier complex has ten data attributes. The purpose of these fields is not to emulate the extensive sets of attributes found in the Global Land Ice Measurements from Space (GLIMS, Raup and Singh Khalsa 2007) database or the WGI, but only to offer convenient locational and identifying information.

RGI20Id

A 14-character identifier of the form RGI20-*rr*.*nnnnn*, where *rr* is the first-order region number and *nnnnn* is an arbitrary identifying code that is unique within the region. These codes were assigned as sequential positive integers at the first-order (not second-order) level, but they should not be assumed to be numbers.

GLIMSId

A 14-character identifier in the GLIMS format G*xxxxxx*E*yyyyy*Θ, where *xxxxxx* is longitude east of the Greenwich meridian in millidegrees, *yyyyy* is north or south latitude in millidegrees, and Θ is N or S depending on the hemisphere. Most of these identifiers were assigned by computing the centroid of the glacier complex, and so are not guaranteed to lie within the glacier complex. They do, however, agree with *CenLon* and *CenLat* (see below).

BgnDate, EndDate

The date of the survey or image from which the outline was taken, in the form *yyyymmdd*, with missing dates represented by -9990000. When a single date is given in the source it is assigned to *BgnDate*. If only a year is given, *mmdd* is set to 0000. Only when the source provides a range of dates is *EndDate* not missing, and in this case the two codes together give the date range.

Slightly fewer than one half of the glacier complexes have date information (Figure 2).

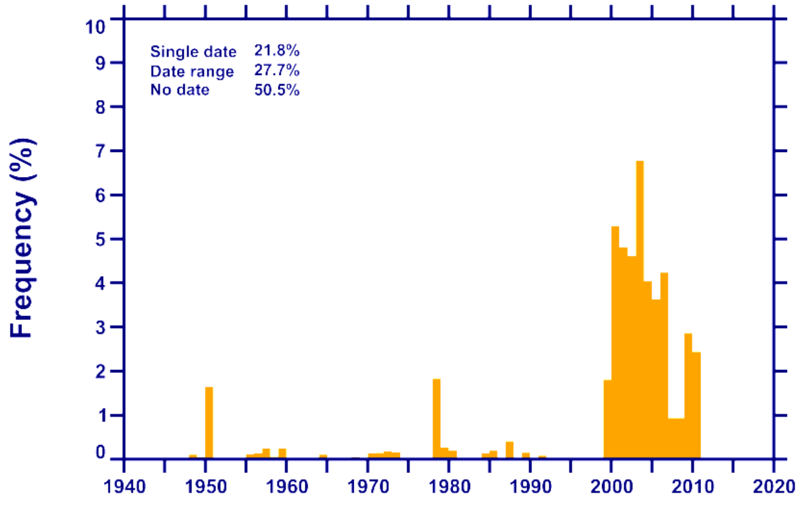

Figure 2. Frequency distribution of dates in RGI version 2.0. Complexes with date ranges are assigned with uniform probability to each year of the range. Most undated complexes were obtained from Landsat ETM+, ASTER or SPOT5 imagery of the 2000s or late 1990s.

CenLon, CenLat

Longitude and latitude, in degrees, of a point representing the location of the glacier complex. Whether or not the point is actually the mathematical centroid, these coordinates agree with those in *GLIMSId*.

O1Region, O2Region
The codes of the first-order and second-order regions (Table 1) to which the glacier complex belongs.

Area
Area of the glacier complex in km^2.

Name
Name of the glacier complex. Nearly all complexes lack this information. However, the 12-character WGI or WGI-XF idcode was inserted here if it was available.

Quality Control
A series of quality checks have been conducted in generating RGI version 2.0 from version 1.0. We began with a check, for each glacier complex, that it conformed to the RGI data model. Not all did. In this model, each complex is a single graphical object consisting of a glacier or glacier-complex outline with clockwise polarity (that is, a polygon with inside on the right looking "downstring") followed immediately by outlines of counterclockwise polarity representing all of the glacier's nunataks.

Each polygon was tested for closure, that is, its last vertex was tested for identity with its first vertex. Unclosed polygons would have been removed, although in fact none were found.

All vertices duplicating their immediately preceding vertices were removed. Duplication means proximity within 2 microdegrees, or about 2 m.

Polygons that were degenerate, or that became degenerate after removal of duplicate vertices, were removed. Degenerate means having fewer than four vertices, the minimum required to represent a triangle.

Glacier complexes with areas less than 0.01 km^2 were removed. Nunataks were retained whatever their area.

The results of this quality-control operation, and of the replacement of some outlines and addition of others, are summarized below for each region under the heading "Changes from Version 1.0 to Version 2.0".

Gridded Data Product
During the generation of version 2.0, each glacier-complex outline was masked onto a 1°×1° global grid in such a way that each cell of the grid acquired its due share of the complex's total area. The final version of the grid thus contained all of the glacierized area in the inventory. The grid also includes the glaciers of Turkey and Chukotka, which are not in the inventory proper.

The grid is provided in RGI version 2.0 as a text file of blank-separated glacierized cell areas in km^2. The file contains 180 rows, ordered from north to south. Each row begins with the latitude of its northern boundary and continues with the 360 glacierized areas for that latitude, beginning at the 180th meridian. Thus, for example, the following pseudocode will read the grid into array G:

```
Real :: G(-180:179,-90:89)
For lat = 89, -90, -1
    Read ( '(4x,360f12.3)' ) G(:,lat)
Next
```

DESCRIPTION OF DATA COMPILATION BY REGION

REGION 1: Alaska

Contributor	Institution	Project/Funding
Arendt, A.	University of Alaska, Fairbanks, USA	National Park Service, Geophysical Institute, NASA Cryospheric Sciences, Geographic Information Network of Alaska
Herreid, S.		
Hock, R.		
Kienholz, C.		
Rich, J.		
Beedle, M.	University of Northern British Columbia, Canada	
Berthier, E.	CNRS-OMP-LEGOS, France	
LeBris, R.	University of Zurich, Switzerland	GlobGlacier funded by ESA
Frey, H.		
Paul, F.		
Bolch, T.		
Burgess, E.	University of Utah, USA	
Forester, R.		
Lund, J.		
Giffen, B.	National Park Service, USA	
Hall, D.	NASA Goddard Space Flight Center, USA	
Manley, W.	INSTAAR, USA	

The Alaska region encompasses all glaciers in the State of Alaska, USA, as well as all glaciers in the Yukon Territory and British Columbia, Canada, that are part of the icefields that straddle the US/Canada Border. On its southeastern boundary, the region ends just north of Prince Rupert, British Columbia and just south of the end of the Alaska border. From there the region extends inland to the divide between Gulf of Alaska and Arctic drainages.

Numerous groups have contributed Alaska glacier outlines. Le Bris et al. (2011) mapped the Kenai Peninsula, Tordillo, Chigmit and Chugach Mountains using Landast TM scenes acquired between 2005-2009. They used automated (band-ratioing) glacier mapping techniques with additional manual editing to deal with incorrect classification of debris-covered glaciers. Drainage divides in the accumulation region were derived from the USGS DEM.

As part of a two-year mapping effort by the National Park Service (NPS), the University of Alaska Fairbanks (UAF) has been mapping all glaciers in NPS boundaries, as well as glaciers connected to but not within park boundaries, for two time periods (USGS 1950s map dates, and most recent satellite imagery). For this effort UAF has in many regions started with existing, older outlines and updated them to the most modern imagery available. These include outlines from Berthier (Berthier et al, 2010), Beedle (Beedle et al, 2007), Giffen, Hall and Manley. UAF has updated these outlines to circa 2010 pan-sharpened 15 m resolution Landsat 7 ETM+ scenes, 5 m resolution imagery from the SPOT SPIRIT initiative (dating approximately 2007; Korona et al., 2009) and 2006-2010 IKONOS imagery. UAF Geophysical Institute internal funding has also been used to support digitizing efforts in the Alaska Range, Chugach Mountains and Juneau Icefield glaciers. Nearly all of these regions are based on 2010 imagery.

The University of Utah (Burgess, Forester, Lund) created outlines for the Stikine Icefield region derived from 1980s Landsat 5 imagery.

Manley provided all outlines for Brooks Range glaciers.

Glaciers along the Aleutian Island chain are taken from Berthier et al (2010). A small (estimated <0.1%) of glaciers in southeast Alaska are taken from Digital Chart of the World outlines.

Glaciers other than those mapped by Le Bris and others (2011) were delineated using an automated algorithm developed by C. Kienholz (manuscript in prep). USGS digital elevation models as well as the ASTER GDEM v1 were used as sources of elevation information for the algorithm.

Changes from Version 1.0 to Version 2.0:

Three glaciers in the Kigluaik Mountains of western central Alaska (01.01) were added as nominal circles from WGI-XF.

Glaciers in Katmai and Lake Clarke National Parks have been updated to 2006-2010 IKONOS imagery.

Portions of the Stikine Icefield region have been improved by removing misidentified small glaciers around the periphery of the icefield.

Glaciers at the head of Lynn Canal, and in the eastern portion of the Western Chugach Mountains near Cordova, have been updated.

Extensive improvements have been made to the Wrangell/St. Elias region. What is included in RGI version 2.0 is a partially edited version of Berthier et al's (2010) and Beedle et al's (2007) outlines, updated to circa 2010 Landsat 7 ETM+ imagery for the Wrangell Mountains, 2006-2010 IKONOS imagery for the US portion of St. Elias, and Canadian topographic maps for the Canadian portion of the St Elias. Between V1.0 and V2.0 we have focused on capturing the largest area changes occurring primarily at low elevations, however some regions remain unmodified between V1.0 and V2.0 (Figure 3).

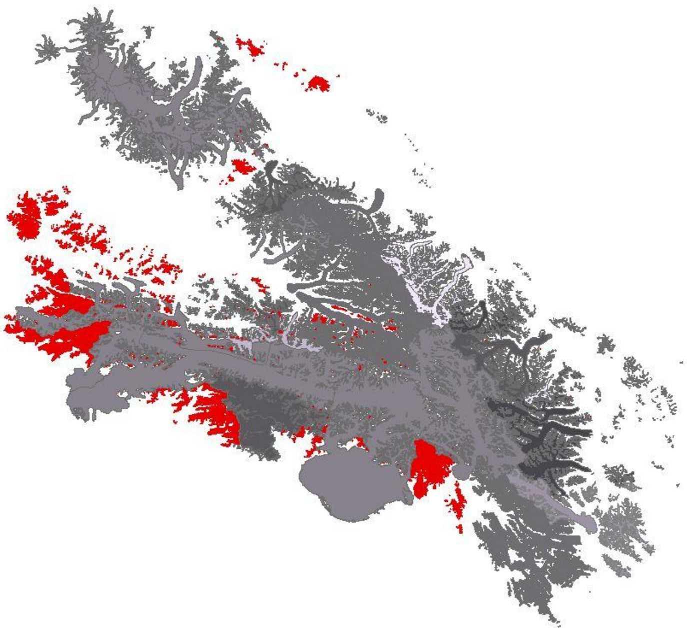

Figure 3: Glaciers of the Wrangell/St.Elias region of Alaska. Red shading indicates areas that have *not yet* been modified between RGI V1.0 and V2.0. Note that some areas in gray still require improvements at high elevations.

REGION 2: Western Canada and US

Contributor	Institution	Project/Funding
Bolch, T.*	UNBC, Canada * now at: University of Zurich, Switzerland	WC2N funded by CFCAS
Menounos, B.		
Wheate, R.		
Fountain, A.	Portland State University, USA	

Glaciers in BC and Alberta were mapped using orthorectified Landsat 5 TM scenes from the years 2004 and 2006 obtained by British Columbia Government, Ministry of Forests and Range. We selected the TM3/TM5 band ratio for glacier mapping. For the entire study area, we used improved British Columbia TRIM glacier outlines as a mask to minimize misclassification due to factors such as seasonal snow. When using this mask, we assumed that glaciers did not advance between 1985 and 2005, an assumption that holds for practically all non-tidewater glaciers in western North America. The mask also maintained consistency in the location of the upper glacier boundary and the margins of nunataks. This consistency is important in case of seasonal snow that hampers correct identification of the upper glacier boundary. We mapped only glaciers larger than 0.05 km^2 as a smaller threshold would include many features that were most likely snow patches. In addition, all snow and ice patches that were not considered to be perennial ice in the TRIM data were eliminated and hence, we minimize deviations in glacier areas that could arise from interpretative errors or major variations in snow cover. The resulting glacier polygons were visually checked for gross errors based on the procedures previously discussed, and overall, fewer than 5% of the glaciers were manually improved. We derived glacier drainage basins based on a flowshed algorithm using the TRIM DEM and a buffer around each glacier. More information can be found in Bolch et al. (2010a).

Data for the remaining US locations were derived from the GLIMS database. Metadata are located at http://glaciers.us.

Changes from Version 1.0 to Version 2.0:

The glaciers on Melville Island (region 02.01) were represented in version 1.0 by DCW outlines and have been replaced by Canvec outlines taken from Region 03. DCW outlines for the Mackenzie Mountains and Selwyn Mountains (region 02.02), on the boundary between Yukon and the North West Territories, were replaced by Canvec outlines provided by M. Sharp and J.G. Cogley.

REGIONS 3 and 4: Arctic Canada North and Arctic Canada South

Contributor	Institution	Project/Funding
Gardner, A.	Clark University, USA	
Wolken, G.	Department of Geological and Geophysical Surveys, Alaska, USA	
Barrand, N.	University of Alberta, Canada	
Cawkwell, F.		
Copland, L.		
Filbert, K.		
Hartmann, G.		
O'Callaghan, P.		
Sharp, M.		
Wyatt, F.		
Burgess, D.	Natural Resources Canada	
Paul, F.	University of Zurich, Switzerland	GlobGlacier funded by ESA

Region 3: Northern Arctic Canada

Glacier outlines were created from late summer, cloud free 1999-2003 Landsat 7 (ETM+) imagery and from 2000-2003 ASTER imagery. A normalized-difference snow index (NDSI) was calculated for all Landsat imagery to classify all snow and ice covered terrain. Empirically derived thresholds were applied to refine these classifications and isolate snow and glacier ice components. A clumping procedure was then applied to the classified snow and ice data to delineate contiguous groups of pixels, followed by an elimination procedure, which removed small non-glacier ice pixels. Gridded snow and ice data were then converted to polygons and edited manually to correct misclassifications. Small portions of some areas within this region were not adequately imaged by Landsat, either due to persistent cloudiness or shadowing. Consequently, in these areas manual (heads-up) digitization of ASTER imagery was used to capture glacier outlines.

Outlines for Devon Island were provided by D. Burgess and were derived from 1999/2000 velocity maps.

Changes from Version 1.0 to Version 2.0:

Canvec outlines of the Melville Island glaciers, which were mistakenly duplicated in region 03 in version 1.0, were transferred to region 02.

Region 4: Southern Arctic Canada

Glacier complex outlines were compiled from 214 CanVec maps, a digital cartographic reference product produced by Natural Resources Canada. An additional 5500 km^2 of glacier area in central Baffin Island not covered by Edition 9 of the CanVec data set were taken from an expanded inventory based on Paul and Kääb (2005) and Svoboda and Paul (2009). All outlines in this expanded inventory were created from late-summer Landsat 7 ETM+ imagery acquired between 1999 and 2002. Of the CanVec maps, 13 were based on late-summer SPOT 5 imagery acquired between 2006-2010 and 7 CanVec on 1958 or 1982 aerial photographs. A small fraction of ice coverage is missed by the Canvec dataset because of incorrect classification over debris covered ice and supraglacial lakes. The misclassification is very noticeable for outlet glaciers where medial moraines are not identified as glacier ice. Glacier complexes were delineated using a basin delineation algorithm developed by

C. Kienholz (manuscript in prep.). Note that these are raw outputs from the delineation algorithm and need to be edited. Users are encouraged to contact RGI data coordinators if they wish to assist in merging and cleaning polygons to improve this dataset.

Changes from Version 1.0 to Version 2.0:

Outlines for 27 glaciers in Labrador (region 04.09) were added, provided by P. O'Callaghan, N. Barrand, F. Wyatt, M. Sharp, University of Alberta.

REGION 5: Greenland Periphery

<table>
<tr><th>Contributor</th><th>Institution</th><th>Project/Funding</th></tr>
<tr><td>Bolch, T.</td><td rowspan="5">University of Zurich, Switzerland</td><td rowspan="5">ice2sea funded by EU FP7
GlobGlacier funded by ESA
Glaciers_cci funded by ESA</td></tr>
<tr><td>Rastner, P.</td></tr>
<tr><td>Moelg, N.</td></tr>
<tr><td>LeBris, R.</td></tr>
<tr><td>Paul, F.</td></tr>
<tr><td>Howat, I.</td><td rowspan="2">Byrd Polar Research Center, Ohio State University, USA</td><td rowspan="2"></td></tr>
<tr><td>Negrete, A.</td></tr>
</table>

There are numerous glaciers in the periphery of the Greenland ice sheet. Distinguishing between what is considered ice sheet versus glaciers is a challenge, and depends on the scientific application. While the distinction is clear for the numerous fully detached glaciers, there are several regions where, although there is a physical connection to the main ice sheet, the ice mass is either a valley glacier in mountainous terrain, or it forms its own ice dome and is largely uncoupled to the ice sheet dynamics. Therefore, for applications such as extrapolation of laser altimetry data, some researchers believe such ice masses should be categorized as glaciers rather than as part of the ice sheet.

The extents that are now provided for RGI 1.0 assign all ice masses with a possible but uncertain drainage divide to the ice sheet (e.g. on the Geikie Plateau), and all others to the local (or peripheral) glaciers and icecaps (GIC). The latter are either:

- not connected to the ice sheet at all
- clearly separable (e.g. by mountain ridges) in the accumulation region, or
- only in contact with ice sheet outlets in the ablation region.

Indeed, there is room for discussion on individual decisions, but for the purpose of the RGI we just need to start somewhere. The individual GIC are currently separated and topographic information is appended. If possible, this information will be included for RGI 2.0. The separation in the accumulation area is done with the drainage divides as derived from DEM-based watershed analysis.

The glaciers in the northern sector of Greenland were not availble from Landsat data and were provided by the Greenland Mapping Project (Howat and Negrete, in prep).

Method (data from Zurich group)

The semi-automated glacier mapping applied to the 64 Landsat scenes that were processed is based on a band ratio (ETM+ band 3 / 5) with an additional threshold in band 1 for better mapping of glacier areas in cast shadow. It is based on Paul and Kääb (2005) and described for a part of western Greenland in Citterio et al. (2009). Debris-covered glacier parts as well as wrongly classified sea ice, ice bergs or lakes were corrected manually in the vector domain. A 3 by 3 median filter is applied for image smoothing and glaciers smaller than 0.05 km^2 are not considered. Wrongly classified regions with seasonal snow could not always be corrected.

Changes from Version 1.0 to Version 2.0:

No changes were made.

REGION 6: Iceland

Contributor	Institution	Project/Funding
Sigurðsson, O.	National Energy Authority, Iceland	

Outlines of glacier complexes in Iceland were added to the GLIMS database by O. Sigurðsson and extracted therefrom by G. Cogley, who merged nunataks with the glacier complexes containing them. Most outlines were acquired from 1999-2004 ASTER and SPOT5 imagery; some in the north of Iceland were acquired from oblique aeriaal photographs.

Changes from Version 1.0 to Version 2.0:

No changes were made.

REGION 7: Svalbard

Contributor	Institution	Project/Funding
Koenig, M. J. Kohler	Norwegian Polar Institute, Norway	Cryoclim funded by ESA
Hagen, J-O.		Cryoclim and Glaciers_cci funded by ESA
Nuth, C.		
Moholdt, G.	University of Oslo, Norway	
Pettersson, R.	Uppsala University, Sweden	

Three primary data sets are used to compile the glacier inventory. The main sources are SPOT5-HRS DEMs and orthophotos provided within the framework of the IPY-SPIRIT (SPOT 5 stereoscopic survey of Polar Ice: Reference Images and Topographies) Project (Korona et al., 2009). The SPOT5-HRS collects 5m panchromatic stereo images that are stereoscopically processed into 40m DEMs, then used for the orthophoto generation of the original images. Five SPIRIT scene acquisitions from 2007-2008 are responsible for covering 71% of the glacier area. The secondary sources are from the ASTER sensor in the form of automatically generated DEMs and orthophotos (AST14DMO products downloaded from NASA). These have a smaller swath width (60 km), and therefore 23 scenes are used to cover 16% of the glacier area. Cloud-free scenes are not available for 2007-2008, and therefore data from as early as 2001 are used. For less than 14% of the glacier area, a suitable SPOT5-HRS or ASTER scene was not available. For these glaciers, 11 orthorectified Landsat scenes are used. Furthermore, additional Landsat and ASTER scenes are used to aid digitization decisions about the seasonal snow cover.

The original glacier delineation and glacier identification system is based on the Hagen et al. (1993) atlas, which conforms to WGI standards but is only available as a hard-copy rather than GIS data. Therefore, digitized national datasets are the base glacier masks from which to begin the inventory (König et. al, in press). From this original dataset, we manually re-delineated the individual glacier basins based upon the Hagen et al. (1993) *Atlas* and updated by trimming the front position and the lateral edges below the ELA. Since the original national dataset was derived by cartographers, much of the mask segments above the ELA contained snow covered valley walls and gullies (not perennially snow covered). These are, to the best of our ability, clipped from the masks by visually analyzing the recent satellite archives of ASTER and Landsat.

Figure 4 summarizes the distribution of imagery dates used to generate the Svalbard outlines.

Changes from Version 1.0 to Version 2.0:

Outlines of the glaciers on Jan Mayen (07.02) were digitized by J.G. Cogley from Hagen et al. (1993).

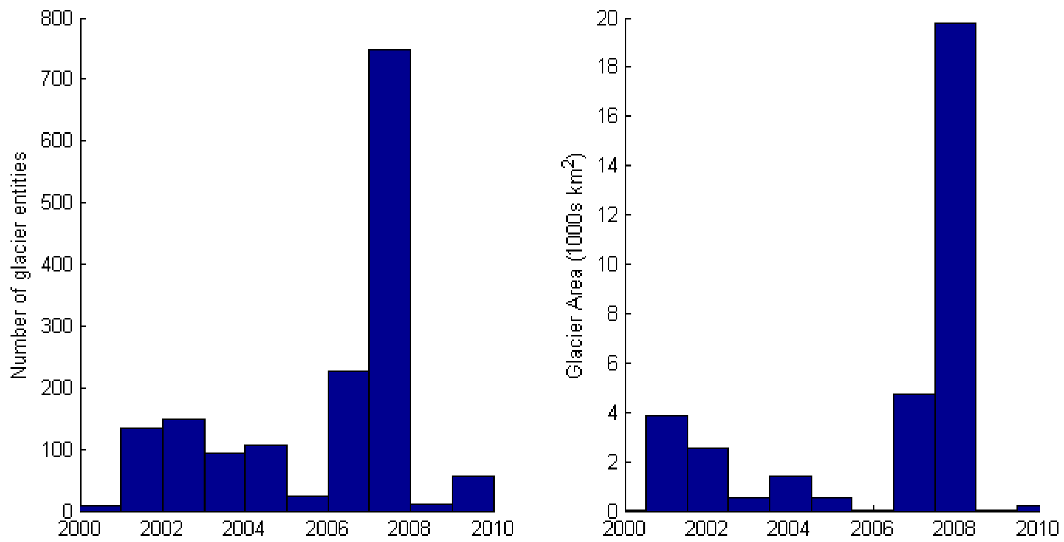

Figure 4. Time distribution of the imagery used to generate the Svalbard portion (Region 7) of the RGI glacier database showing the number of glaciers (left) and the total glacier area (right) as a function of image year.

REGION 8: Scandinavia

Contributor	Institution	Project/Funding
Andreassen, L.	Norwegian Water Resources and Energy Directorate, Norway	
Winsvold, S.		
Hagen, J-O.	University of Oslo, Norway	
Paul, F.	University of Zurich, Switzerland	GlobGlacier funded by ESA
Mercer, A.	University of Stockholm, Sweden	
Brown, I.		

The glacier outlines for Norway are based on Landsat (TM and ETM+) imagery from 1999-2006.

The Swedish glacier outlines use imagery from SPOT5 and SPOT4 (dates not provided). In some regions these outlines were updated against September 2008 Swedish Land Survey imagery available on Google Earth.

The glacier mapping to which GlobGlacier contributed is documented in Andreassen et al. (2008) for Jotunheimen, Paul and Andreassen (2009) for Svartisen, and Paul et al. (2011) for the Jostedalsbreen region.

Changes from Version 1.0 to Version 2.0:

Four glaciers in the Khibiny Mountains of the Kola Peninsula (08.02) were added as nominal circles from WGI-XF.

REGION 9: Russian Arctic

Contributor	Institution	Project/Funding
Moholdt, G.	University of Oslo, Norway	ice2sea, grant number 226375

This basic inventory was constructed as a part of a mass balance study of the Barents/Kara Sea region in the Russian High Arctic (Moholdt et al., submitted). It covers all glaciers and ice caps in Novaya Zemlya (22,100 km^2), Severnaya Zemlya (16,400 km^2), Franz Josef Land (12,700 km^2), Ushakov Island (320 km^2) and Victoria Island (6 km^2). Glacier complexes were manually digitized from orthorectified satellite imagery acquired during summers between 2000 and 2010. SPIRIT SPOT5 scenes (Korona et al, 2009) were used for most of Novaya Zemlya, while the best available Landsat scenes were used elsewhere. All visible nunataks were cut out from the glacier polygons, and snowfields were only included if they seemed to be a part of a glacier. Ice shelves in Franz Josef Land (<50 km^2) were included as parts of the glacier polygons, while the Matusevich Ice Shelf in Severnaya Zemlya (~200 km^2) was delineated into a separate polygon. The estimated total glacier area of the region (51,500 km^2) is 9% smaller than that of the World Glacier Inventory (Ohmura, 2009). This large deviation is probably due to a combination of long-term glacier retreat and methodological differences in glacier delineation.

Changes from Version 1.0 to Version 2.0:

The Matusevich Ice Shelf, which would have been the only ice shelf in the inventory, was removed.

REGION 10: North Asia

Contributor	Institution	Project/Funding
Stokes, C., Gurney, S.	Durham University, UK	
Khromova, T.	Institute of Geography, Russian Academy of Science, Moscow, Russia	

About one third of the glacier outlines in North Asia were manually delineated from Landsat TM/ETM+ or ASTER imagery. Missing areas were filled by a glacier layer compiled by B. Raup (Raup et al., 2000) from the Digital Chart of the World (DCW) and the World Glacier Inventory (WGMS, 1989; Haeberli et al., 1998). The DCW includes layers of geographic information covering the whole world, is based on the United States Defense Mapping Agency's Operational Navigation Charts, and includes a GIS coverage of land ice.

The WGI data base locates each glacier with only a single geographical coordinate rather than a polygon. These glaciers are presented as approximately circular polygons of the area given in the WGI.

Changes from Version 1.0 to Version 2.0:

The DCW outlines of glacier complexes in Mongolia were replaced by outlines of glaciers (not glacier complexes) digitized by J.G. Cogley from Soviet military maps. Their dates range between 1968 and 1983.

14 glaciers in the Tajgonos Peninsula, northwest of Kamchatka (10.02) were added as nominal circles from WGI-XF.

The information available for Chukotka (10.02 and 10.03 ; Sedov 1997) did not include locations of individual glaciers, but their total area of 17.1 km^2 was added to the 10 cells that they occupy in the 1°×1° grid.

REGION 11: Central Europe

Contributor	Institution	Project/Funding
Frey, H.	University of Zurich, Switzerland	GlobGlacier funded by ESA
LeBris, R.		
Paul, F.		

The glacier outlines for this region are derived from ten Landsat TM images acquired during 2 months in the summer of 2003 using band ratio images. Drainage divides for individual glaciers were derived from the void-filled SRTM DEM (from CGIARS) in a resampled version with 60 m spatial resolution. All further details are documented in Paul et al. (2011b). About 30-50 km^2 of glaciers are not mapped, mainly very small glaciers located in Italy (Brenta and Dolomites) and Germany, covered by debris or located under local orographic clouds. A more complete version is planned for the RGI 2.0. The original data sets (in UTM projection) can be downloaded from the globglacier.ch website (link Data access).

Changes from Version 1.0 to Version 2.0:

109 glaciers in the Pyrenees, and one in the Apennines, were added as nominal circles from WGI-XF. Together they constitute region 11.02.

REGION 12: Caucasus and Middle East

Contributor	Institution	Project/Funding
Khromova, T.	Institute of Geography, Russian Academy of Science, Moscow, Russia	

The Caucasus is covered by the database of the Global Land Ice Measurements from Space initiative (GLIMS) (Raup et al., 2007).

Changes from Version 1.0 to Version 2.0:
The 37 glaciers of Iran (12.02) were added from Moussavi et al. (2009).

The information available for Turkey (Kurter 1991) was not adequate for placing the individual glaciers, which have a total area of 22.9 km^2. This area was however added to the 11 Turkish glacierized cells of the 1°×1° grid.

REGION 13: Central Asia

Contributor	Institution	Project/Funding
Bolch, T.	Technische Universität Dresden, Germany; University of Zurich, Switzerland	DynRG-TiP and Aksu-Tarim-RS funded by the German Research Foundation (DFG)
Moelg, N.		
Kriegel, D.	GFZ Potsdam, Germany	CAWa, German Federal Foreign Office
Hagg, W.	LMU Munich, Germany	
Mayer, C.	Commission for Glaciology, Munich	
Khromova, T.	Institute of Geography, Russian Academy of Science, Moscow, Russia	

Large parts of Central Asia are covered by the database of the Global Land Ice Measurements from Space initiative (GLIMS). The GLIMS database consists in China of data from the first Chinese glacier inventory (Shi et al., 2009) and is of heterogeneous and generally slightly lower quality (more generalized) than the other glacier data used here. It has also to be noted that some of the GLIMS data in Central Asia have a shift in location. Large parts of the Tien Shan in Kazakhstan and Kyrgyzstan were mapped semi-automatically using ratio images from ASTER data (e.g. Kutusov and Shahgedanova, 2009). Important missing areas such as the Central Pamirs, Naryn basin, northern Tien Shan (Bolch, 2007) and the Dzungar Alatau were mapped semi-automatically with manual corrections using Landsat TM/ETM+ scenes. The glacier inventory for the Nyainqentanglha Range in Tibet were provided by Bolch et al. (2010b).

Remaining missing areas were filled by a glacier layer compiled by B. Raup (Raup et al., 2000) from the Digital Chart of the World (DCW) and the World Glacier Inventory (WGMS, 1989; Haeberli et al., 1998). The DCW data includes layers of geographic information covering the whole world, is based on the United States Defense Mapping Agency's Operational Navigation Charts, and includes a GIS coverage of land ice.

The WGI data base locates each glacier with only a single geographical coordinate rather than a polygon. These glaciers are presented as approximately circular polygons of the area given in the WGI.

Changes from Version 1.0 to Version 2.0:

No changes were made.

REGION 14 and 15: South Asia West and South Asia East

Contributor	Institution	Project/Funding
Bolch, T.	University of Zurich, Switzerland	GlobGlacier funded by ESA
Frey, H.		
Paul, F.		
Bajracharya, S.	ICIMOD, Nepal	
R. Bhambri	Center for Glaciology, Wadia Institute of Himalayan Geology, Dehradun India	

Large parts of the Himalaya, Karakoram and Pamir are covered by the database of the Global Land Ice Measurements from Space initiative (GLIMS) (Raup et al., 2007). For the present study, GLIMS data was used in cases where no other data was available, mainly on the northern slopes of the Himalayas and the northeastern part of Karakoram. In these regions, the GLIMS database consists mostly of data from the first Chinese glacier inventory (Shi et al., 2009) and is of heterogeneous and generally slightly lower quality than the other glacier data used here. Glacier outlines compiled by the International Centre for Integrated Mountain Development (ICIMOD) were used for large parts of the Karakoram, as well as the central and eastern Himalayas (ICIMOD, 2007, DVD). For Nepal, more recent data from 2008 and 2009 is available and was used here (ICIMOD, 2011, DVD). For large parts of northwestern India, glacier inventory data compiled by the GlobGlacier project of the European Space Agency (ESA) (Paul et al., 2009) was used; the information was compiled from Landsat ETM+ and ALOS PALSAR data (Frey et al., in rev.). For a few regions in the Karakoram Range, no suitable glacier data was available. We therefore compiled new glacier outlines in these regions based on Landsat ETM+ data from the years 2002, 2009, and 2010.

Changes from Version 1.0 to Version 2.0:

Six glaciers in the Ghorband River basin, Afghanistan (14.01) were added as nominal circles from WGI-XF. The Ghorband is one of the headwaters of the Kabul River and thus of the Indus. It is possible that more Afghan glaciers remain to be identified further to the southwest (Shroder and Bishop 2010).

REGION 16: Low Latitudes

Contributor	Institution	Project/Funding
Sharp, M.	University of Alberta, Canada	
Wyatt, F.		
Miles, E.	University of British Columbia, Canada	

In South America, shapefiles were created from late summer, cloud free Landsat 7 ETM+ imagery acquired prior to the 2003 scan line corrector (SLC) failure. To identify glacier surfaces, a normalized difference snow index (NDSI) was calculated using bands 5 and 2 for the red and near-infrared bands respectively. A threshold of approximately 0.5-0.65 was used to identify dirty/shady/bare ice, and one from 0.65-0.99 to identify snow-covered ice. Gridded files were then converted to polygons and additional manual editing was carried out to eliminate incorrectly classified regions.

Changes from Version 1.0 to Version 2.0:

Outlines of the glaciers of Mexico (16.02) were digitized by J.G. Cogley from maps in White (2002).

59 glaciers in east Africa (16.03) and seven in New Guinea (16.04) were added as nominal circles from WGI-XF.

Summary of quality controls conducted by E. Miles, University of British Columbia:

1. Version 1.0 RGI shapefile topology was corrected, splitting the single polygon into individual glacier polygons (total of 14167 polygons).
2. Using the ice flowshed delineation script developed by C. Kienholz (UAF), the glacier polygons were divided into expected ice drainages. This processing preserved the original area of 5066.1 km^2 (measured in UTM 18S) and resulted in 16255 polygons.
3. All polygons smaller than 0.01 km^2 were then removed. A survey of these polygons showed that the vast majority were isolated and contained only 3 or 4 vertices. These small polygons (9869 in number) encompassed a total area of 20.8 km^2, again measured in UTM 18S.
4. The remaining 6386 polygons were individually inspected in ArcGIS with a standard ESRI satellite image basemap to remove gross inaccuracies.
    1. Due to difficulties in obtaining minimum-snow satellite imagery for the NDSI calculation used to create the initial dataset, there was significant snow contamination in the glacier dataset. The most obvious problems occurred in the severely arid regions of southern Peru and northern Chile, although problems were also evident in the temperate zones.
    2. Each polygon was inspected with consideration for the basemap satellite imagery, with scale fixed at 1:50,000 unless specific outlines warranted further inspection.
        1. Glacier outlines which were snow-covered or obscured by clouds in the basemap imagery were preserved as-is.
        2. Many glacier outlines encompassed both snow and rock (or vegatation, etc). If the snow portion was substantial (over a third or distributed over the entire outline), the outline was left as-is. If snow encompassed a very small and concentrated portion of the polygon, the polygon was roughly trimmed to this extent.
        3. Only glaciers containing no snow cover, where a debris-covered glacier was also implausible, were removed in their entirety.
    3. The resulting dataset included 4382 glacier outlines and 4088.2 km^2.
5. This inspection revealed an odd spatial shift for all polygons in a contiguous region between

approximately Huaraz, Peru, and Conchucon, Peru. The features did not properly align with mountains evident in the ArcMap satellite imagery or in Google Earth. Most of the features appeared to be shifted by approximately 1.2km North of the mountains that they matched, and a zone near Huaraz show duplicated features in the outlines - one set of glaciers mapping correctly over the mountains with a matching set of features located about to the 1.2 km North. Likely due to an incorrect spatial representation of one of the source images used in the original glacier demarcation, the misregistration would be problematic for modelling.

1. All glacier outlines within this region were extracted from the entire dataset (and deleted from the original). Individually, each glacier complex was uniformly shifted approximately 1.2km South, then adjusted to provide the best fit with topography and the satellite imagery backdrop. Since the required transformation was not quite linear (more shift was required for the northernmost outlines) it is likely that the source image had some minor distortion associated with the misregistration.

2. The duplicate features were then manually trimmed (coarsely) according to a combination of the two outlines available in conjunction with the satellite image backdrop.

3. After a satisfactory shift had been imposed, the individual glacier outlines were merged to a single polygon, and re-run through Christian's ice flowshed delineation script, such that the outlines would represent ice divides according to the correct topography.

4. The corrected outlines were then merged back to the larger dataset and seams were trimmed where the polygons intersected.

6. The resulting dataset (attached) contains a total of 4373 outlines and covers an area of 4057.1 km^2.

7. Having inspected each polygon, I would estimate that a more rigorous examination and delineation of each glacier would result in a further area reduction of up to 20%. Many outlines extend well beyond the terminus implied by the satellite imagery I could source, by my objective was primarily to remove the outlines that obviously did not represent glaciers at all.

REGION 17: Southern Andes

Contributor	Institution	Project/Funding
Sharp, M.	University of Alberta, Canada	
Wyatt, F.		
Miles, E.	University of British Columbia, Canada	
De Angelis, H.	Stockholm University, Sweden	

Shapefiles were created from late summer, cloud free Landsat 7 ETM+ imagery acquired prior to the 2003 SLC failure. To identify glacier surfaces, a normalized difference snow index (NDSI) was calculated using bands 5 and 2 for the red and near-infrared bands respectively. A threshold of approximately 0.5-0.65 was used to identify dirty/shady/bare ice, and one from 0.65-0.99 to identify snow-covered ice. Gridded files were then converted to polygons and additional manual editing was carried out to eliminate incorrectly classified regions.

Shapefiles for the South Patagonian Icefield were provided by De Angelis (submitted).

Changes from Version 1.0 to Version 2.0:

Summary of quality controls conducted by E. Miles, University of British Columbia:

1. The original RGI shapefile's topology was corrected, splitting the single polygon into individual glacier polygons (total of 42397 polygons covering 33786 km2).
2. All polygons smaller than 0.01 square kilometers were then removed. A survey of these polygons showed that (as in the Northern Andes) the vast majority were isolated and contained only 3 or 4 vertices. These small polygons (26396 in number) encompassed a total area of 59.23 km2, measured in UTM 18S.
3. The remaining 16001 polygons were individually inspected in ArcGIS and compared to a standard ESRI satellite image basemap and a Bing Maps satellite basemap to remove gross inaccuracies. The Bing basemap was used primarily for areas where the ESRI image included substantial cloud cover. The two basemaps were qualitatively compared in cloud-free regions and the agreement was deemed satisfactory for the removal of blatantly erroneous data. For highly ambiguous zones, Google Earth was utilized as a third image and rough terrain dataset to help interpret the satellite images and glacier outlines.
    1. Due to difficulties in obtaining minimum-snow satellite imagery for the NDSI calculation used to create the initial dataset, there was significant snow contamination in the glacier dataset. This problem was most particularly in southern Patagonia. The Cordillera de Darwin and the ranges east of the Icefields often included snowlines rather than glacier outlines. Additionally, debris-covered glaciers and water-terminating glacial tongues posed significant problems for the NDSI algorithm. Finally, the utilization of Landsat-7 data inappropriately blended with Landsat-5 data led to substantial stripe patterns in some areas (different sampling dates resulted in a changed snowline between the striped L7 data and the solid L5 data).
    2. Each polygon was inspected with consideration for the basemap satellite imagery, with scale fixed at 1:60,000 unless specific outlines warranted further inspection.
        1. Glacier outlines which were snow-covered or obscured by clouds in all the basemap imagery were preserved as-is.
        2. Many glacier outlines encompassed both snow and rock (or vegatation, etc). If the snow portion was substantial (over a third or distributed over the entire outline), the outline was left as-is. If snow encompassed a very

        small and concentrated portion of the polygon, the polygon was roughly trimmed to this extent.
        3. Striping due to L5/L7 blending was edited where possible.
        4. Many glacier outlines included peripheral zones that were implausible as connected zones of deforming ice, but realistically could include small glacierets or other perennial ice cover. This zones were eliminated where possible as per 3.2.2, but were often left in the dataset.
        5. Only glaciers containing no snow cover where a debris-covered glacier was also implausible (lakes, vegetated slopes, snow-banked streams, etc), were removed in their entirety.
        6. Water-terminating glacier tongues were often enlarged to cover the extent shown in the satellite imagery. Debris exposed as the gonue melts seemed to frustrate the algorithm. The same issue occurred with larger land-terminating glaciers whose tongues had accumulated significant debris.
        7. Debris-covered glaciers were in some cases omitted in their entirety by the dataset. Where observed, a rough outline of the glacier was added according to the three imagery datasets. I estimate adding 20-25 such glacier outlines, primarily between 33.5 and 34.5 degrees South.
    3. The resulting dataset included 14014 glacier outlines.
4. The next step was to incorporate the glacier outlines for the Lagos region of Chile and Argentina, developed by Frank Paul.
    1. The extent of the source scenes was not perfectly clear, but Frank Paul's dataset was assumed to accurately contain all glacier outlines East-West across the Andes for it's entire North-South extent.
    2. At the southern margin of this dataset, two glacier outlines had straight-line southern edges - these were take as outlines falling on the satellite image's edge, and corresponded directly to RGI outlines that continued further South. These overlapping outlines were combined.
5. The combined dataset (edited RGI and Frank Paul's outlines) were then processed according to Christian Kienholz's flowshed delineation algorithm.
6. The next step was to incorporate Hernan de Angelis' outlines for the South Patagonian Icefield:
    1. All outlines that intersected the prior-version South Patagonian Icefield polygon (which blended into adjacent ranges due to snowline outlines) were extracted from my recent edited dataset.
    2. These outlines were then intersected with Hernan's outlines, creating a dataset containing his exact outlines and the leftover parts of my outlines for this region, split by flowsheds. These polygons were examined individually with respect to the same basemaps identified above:
        1. Polygons sourced from Hernan's dataset were left as-is.
        2. Polygons which appeared separated from the icefield were left as-is.
        3. Exception: Sliver polygons removed from the icefield were removed when it was clear that my edit did not correspond to a realistic flowshed.
        4. Polygons adjacent to the icefield were included when the basemap appeared as though an independent flowshed actually existed.
        5. Polygons adjacent to the icefield were sometimes thin slivers (my edited extent differed from Hernan's). These excess slivers resulting from my dataset were removed.
    3. This dataset was then merged with the Frank Paul and edited RGI outlines described above.

7. The final dataset (attached) contains 17438 glacier outlines, covering a total area of 32558 km2.
8. While the SouthernAndes only exhibited a change of 1000km2 of coverage as the result of this editing process, the improvements were much more extensive than for the Low-latitude Andes:
    1. Substantial reductions in area due to the elimination of false-positive area (lakes, snow, or vegetation cover included in glacier outlines) were largely offset by inclusion of false-negative area (debris-covered glaciers and water-terminating tongues). Via intermediate datasets I estimate the elimination of more than 2000km2 of false-positive area before the inclusion of 1000km2 of false-negative area.
    2. Where possible, eliminations of area led to much more realistic glacier outlines, rather than a fractured landscape. There are still substantial gains to be made in this realm, but those gains would require much more extensive efforts.
    3. I estimate 5% error by area remains in the dataset, mostly as glacier-peripheral snow and transient ice, which is clearly evident in examination of the outlines. Since one connected ice mass (N. Pat. Icefield) contains ~50% of the region's ice area, peripheral areas are minor on a percent-areal basis, but may be 100s of km2.
    4. I believe that this dataset is on the whole a conservative area estimate, having accounted for nearly all of the false-negative zones.

REGION 18: New Zealand

Contributor	Institution	Project/Funding
Chinn, T.	Canterbury University, NZ	

New Zealand outlines are derived from 1978 aerial imagery at a scale of 1:150,000 as used for the NZ Topo50 maps (Chinn, 2001). The shapefile can be downloaded from:

http://data.linz.govt.nz/#/layer/287-nz-mainland-ice-polygons-topo-150k/

Changes from Version 1.0 to Version 2.0:

No changes were made.

REGION 19: Antarctic and Subantarctic

Contributor	Institution	Project/Funding
Bliss, A.	University of Alaska, Fairbanks, USA	
Hock, R.		
LeBris , R.	CNRS-OMP-LEGOS, France	
Berthier, E.		
Cogley, G.	Trent University, Canada	

Outlines of glacier complexes on islands peripheral to the mainland of Antarctica were obtained from the Antarctic Digital Database (ADD Consortium, 2000). A. Bliss manually classified the ADD's "land" polygons into continent, ice rise, ice cap, and glacier complex polygons. Continental ice areas and ice rises are not included in this inventory. The classification was based on the surface morphology and surface flow velocities observed in data from Landsat, RADARSAT Antarctic Mapping Project DEM, and MEaSUREs InSAR-Based Antarctic Velocity Map. For islands with prominent nunataks, glacier complexes were subdivided into individual glaciers using a semi-automated algorithm developed by C. Kienholz (manuscript in prep.).

Outlines of glaciers on the Subantarctic islands were obtained by G. Cogley from various sources including satellite imagery and maps. For King George Island in the South Shetland Islands, outlines were downloaded from KGIS, the King George Island Geographic Information System, a now defunct web site created by F. Rau and S. Vogt, University of Freiburg. Separate outlines of "glacier basins" and ice-free areas were harmonized and merged to form glacier outlines containing nunataks. For Kerguelen, outlines are from Berthier et al. (2009). Outlines of South Georgia glaciers have been mapped by F. Paul from a Landsat ETM+ scene from 2003 using a band 3/5 ratio and manual corrections for icebergs and water (removed), and debris-cover (added); some regions covered by seasonal snow might be included and will be removed for the RGI 2.0.

Changes from Version 1.0 to Version 2.0:

The ice cover of Peter the First Island in the Bellingshausen Sea was taken from the ADD in version 1.0. In version 2.0 it is replaced by the outlines of 26 glaciers from an inventory by J.G. Cogley (Cogley et al., in press).

0 No significant calving

1 Terrestrial ("dry") calving

2 Marine calving

3 Lacustrine calving

4 Ice shelf (AKB added)

Quote from Bliss, Hock, Cogley Annals of Glaciology paper draft (2012):

"The first four correspond to the classification in Cogley (2008); the last is unique to Antarctica. Classification was done visually using imagery from a variety of sources, found in Google Earth (as of

21 March 2012). In a few instances, more than one category applied to a particular glacier. Each of these glaciers was assigned to the class representing the longest part of its perimeter."

REFERENCES

ADD Consortium (2000), *Antarctic Digital Database, Version 3.0, Database, Manual and Bibliography*. Scientific Committee on Antarctic Research, Cambridge. 93p and digital data (version 4.1; http://www.add.scar.org/add_main.html).

Andreassen, L.M., F. Paul, A. Kääb, and J.E. Hausberg (2008), Landsat-derived glacier inventory for Jotunheimen, Norway, and deduced glacier changes since the 1930s, *The Cryosphere*, 2, 131-145.

Beedle, M., M. Dyurgerov, W. Tangborn, S. Khalsa, C. Helm, B. Raup, R. Armstrong, and R. Barry (2008), Improving estimation of glacier volume change: a GLIMS case study of Bering Glacier System, Alaska, *The Cryosphere*, 2, 33-51.

Berthier, E., R. Le Bris, L. Mabileau, L. Testut, and F. Rémy (2009), Ice wastage on the Kerguelen Islands(49S, 69E) between 1963 and 2006, *Journal of Geophysical Research*, 114 (F3), doi:10.1029/2008JF001192.

Berthier, E., E. Schiefer, G. Clarke, B. Menounos, and F. Rémy (2010), Contribution of alaskan glaciers to sea level rise derived from satellite imagery, *Nature Geoscience*, 3, 92-95, doi:10.1038/NGEO737.

Bolch, T. (2007), Climate change and glacier retreat in northern Tien Shan (Kazakhstan/Kyrgyzstan) using remote sensing data, *Global and Planetary Change, 56,* 1–12.

Bolch, T., B. Menounos, and R.D. Wheate (2010a), Landsat-based inventory of glaciers in western Canada, 1985 - 2005, *Remote Sensing of Environment, 114*(1), 127–137.

Bolch, T., T. Yao, S. Kang, M.F. Buchroithner, D. Scherer, F. Maussion, E. Huintjes, and C. Schneider (2010b), A glacier inventory for the western Nyainqentanglha Range and Nam Co Basin, Tibet, and glacier changes 1976-2009, *The Cryosphere,* 4, 419–433.

Cogley, J.G., 2009, A more complete version of the World Glacier Inventory, *Annals of Glaciology*, **50**(53), 32-38.

Cogley, J.G., E. Berthier and S. Donoghue, in press, Glaciers of the Subantarctic islands, in Kargel, J.S., M.P. Bishop, A. Kääb, B. Raup and G. Leonard, eds., *Global Land Ice Measurements from Space: Satellite Multispectral Imaging of Glaciers*, Praxis-Springer.

Chinn, T.J. (2001), Distribution of the glacial water resources of New Zealand, *Journal of Hydrology*, 40 (2), 139-187.

Citterio, M., F. Paul, A.P. Ahlstrøm, H.F. Jepsen, and A. Weidick (2009): Remote sensing of glacier change in West Greenland: accounting for the occurrence of surge-type glaciers, *Annals of Glaciology*, 50(53), 70-80.

Danko, D.M. (1992): The digital chart of the world project, *Photogrammetric Engineering and Remote Sensing*, 58(8), 1125 – 1128.

De Angelis (*submitted*): Hypsometry and sensitivity of glaciers to changes in equilibrium line altitude: the case of the South Patagonian Icefield.

Frey, H., F. Paul, and T. Strozzi (in revision), Compilation of a glacier inventory for the western Himalayas from satellite data: Methods, challenges and results, *Remote Sensing of Environment*.

Haeberli, W., M. Hoelzle, and S. Suter, eds., 1998, *Into the Second Century of World-Wide Glacier Monitoring – Prospects and Strategies*, UNESCO, Paris.

Hagen, J. O., O. Liestøl, E. Roland, and T. Jørgensen (1993), Glacier Atlas of Svalbard and Jan Mayen, *Norsk Polarinstitutt Meddelelser,* Nr. 129, Oslo.

Howat, I.M and A. Negrete (in prep.), A high-resolution ice mask for the Greenland Ice Sheet and peripheral glaciers and icecaps. http://bprc.osu.edu/GDG/icemask.php**.**

ICIMOD (2007), Inventory of glaciers, glacial lakes and identification of potential glacial lake outburst floods (GLOFs), Affected by Global Warming in the Mountains of Himalayan Region (Kathmandu, 2007).

ICIMOD (2011), Glacial lakes and glacial lake outburst floods in Nepal – additional material (ICIMOD, Kathmandu, 2011).

ICIMOD (2011), The Status of Glaciers in the Hindu Kush-Himalayan Region, Bajracharya, S., and B. Shrestha eds. International Centre for Integrated Mountain Development, Kathmandu, Nepal.

König, M., Nuth, C., Kohler, J., Moholdt, G., and Pettersen, R. (in press), A digital glacier database for Svalbard, in Kargel, J.S., M.P. Bishop, A. Kääb, B. Raup and G. Leonard, eds., *Global Land Ice Measurements from Space: Satellite Multispectral Imaging of Glaciers*, Praxis-Springer..

Korona, J., Berthier, E., Bernard, M., Rèmy, F., and Thouvenot, E.: SPIRIT. SPOT 5 stereoscopic survey of Polar Ice (2009), Reference Images and Topographies during the fourth International Polar Year (2007-2009), *ISPRS Journal of Photogrammetry and Remote Sensing*, 64, 204-212.

Kutuzov, S., and M. Shahgedanova (2009), Glacier retreat and climatic variability in the eastern Terske-Alatoo, inner Tien Shan between the middle of the 19th century and beginning of the 21st century, *Global and Planetary Change,* 69(1-2), 59–70.

Kurter, A., 1991, Glaciers of Turkey, in Williams, R.S., Jr., and J.G. Ferrigno, eds., *Satellite Image Atlas of Glaciers of the World*, U.S. Geological Survey Professional Paper 1386-G, 1-30.

Le Bris, R., F. Paul, H. Frey, and T. Bolch (2011), A new satellite-derived glacier inventory for western Alaska, *Annals of Glaciology*, 52 (59), 135-143.

Liu, H., K. Jezek, B. Li, and Z. Zhao. (2001), *Radarsat Antarctic Mapping Project digital elevation model version 2*. Boulder, CO: National Snow and Ice Data Center. Digital media.

Moholdt, G., B. Wouters B., and A. Gardner (submitted), Recent mass changes of glaciers in the Russian High Arctic.

Moussavi, M.S., M.J. Valadan Zoej, F. Vaziri, M.R. Sahebi and Y. Rezaei, 2009, A new glacier inventory of Iran, *Annals of Glaciology*, **50**(53), 93-103.

Ohmura, A. (2009), Completing the World Glacier Inventory, *Annals of Glaciology,* 50(53), 144-148.

Paul, F. and A. Kääb (2005), Perspectives on the production of a glacier inventory from multispectral satellite data in the Canadian Arctic: Cumberland Peninsula, Baffin Island, *Annals of Glaciology*, 42, 59-66.

Paul, F. and L.M. Andreassen (2009), A new glacier inventory for the Svartisen region, Norway, from Landsat ETM+ data: challenges and change assessment, *Journal of Glaciology*, 55 (192), 607-618.

Paul, F., L.M. Andreassen, and S.H. Winsvold (2011a), A new glacier inventory for the Jostedalsbreen region, Norway, from Landsat TM scenes of 2006 and changes since 1966, *Annals of Glaciology*, 52 (59), 153-162.

Paul, F., H. Frey, and R. Le Bris (2011b), A new glacier inventory for the European Alps from Landsat TM scenes of 2003: Challenges and results, *Annals of Glaciology*, 52 (59), 144-152.

Raup, B., and S.J. Singh Khalsa, 2007, *GLIMS Analysis Tutorial*, http://glims.org. 8p.

Raup, B., H. Kieffer, T. Hare, and J. Kargel (2000), Generation of data acquisition requests for the ASTER satellite instrument for monitoring a globally distributed target: Glaciers, *IEEE Transactions on Geoscience and Remote Sensing,* 38, 1105–1112.

Raup, B., A. Kääb, J.S. Kargel, M. P. Bishop, G. Hamilton, E. Lee, F. Paul, F. Rau, D. Soltesz, S.J. Khalsa, et al. (2007), Remote sensing and GIS technology in the global land ice measurements from space (GLIMS) project, *Computers and Geosciences*, 33 (1), 104-125.

Rignot, E., J. Mouginot, and B. Scheuchl. (2011), Ice Flow of the Antarctic Ice Sheet, *Science*, 333(6048), 1427-1430. doi 10.1126/science.1208336.

Sedov, R.V., 1997, Ledniki Chukotki, *Materialy Glyatsiologicheskikh Issledovaniy*, **82**, 213-217.

Shi, Y., C. Liu, and E. Kang (2009), The Glacier Inventory of China, *Annals of Glaciology 50*(53), 1–4.

Shroder, J.F., Jr., and M.P. Bishop, 2010, Selected glaciers of Afghanistan, in Williams, R.S., Jr., and J.G. Ferrigno, eds., *Satellite Image Atlas of Glaciers of the World – Asia*, U.S. Geological Survey Professional Paper 1386-F, 167-199. U.S. Government Printing Office, Washington, D.C.

Svoboda, F. and F. Paul (2009), A new glacier inventory on southern Baffin Island, Canada, from ASTER data: I. Applied methods, challenges and solutions, *Annals of Glaciology*, 50 (53), 11-21.

WGMS (1989): World glacier inventory - Status 1988. Haeberli, W., Bösch, H., Scherler, K., Østrem, G. and Wallén, C. C. (eds.), IAHS (ICSI) / UNEP / UNESCO, World Glacier Monitoring Service, Zurich, Switzerland: 458 pp.

White, S.E., 2002, Glaciers of Mexico, in Williams, R.S., Jr., and J.G. Ferrigno, eds., *Satellite Image Atlas of Glaciers of the World – North America*. U.S. Geological Survey Professional Paper 1386-J, 383-405. U.S. Government Printing Office, Washington, D.C.